

Article

Characterization of a Novel Nicotine Hydroxylase from *Pseudomonas* sp. ZZ-5 That Catalyzes the Conversion of 6-Hydroxy-3-Succinoylpyridine into 2,5-Dihydroxypyridine

Tao Wei ¹, Jie Zang ¹, Yadong Zheng ¹, Hongzhi Tang ², Sheng Huang ¹ and Duobin Mao ^{1,*}

¹ School of Food and Biological Engineering, Zhengzhou University of Light Industry, Zhengzhou 450002, China; weit8008@zzuli.edu.cn (T.W.); zangjie@163.com (J.Z.); Zhengyud@163.com (Y.Z.); Huangshen@126.com (S.H.)

² State Key Laboratory of Microbial Metabolism, School of Life Sciences and Biotechnology, Shanghai Jiao Tong University, Shanghai 200240, China; Tanghz@126.com

* Correspondence: duobinmao@126.com; Tel.: +86-371-86609631; Fax: +86-371-86609631

Received: 11 August 2017; Accepted: 26 August 2017; Published: 31 August 2017

Abstract: A novel nicotine hydroxylase was isolated from *Pseudomonas* sp. ZZ-5 (HSPH_{ZZ}). The sequence encoding the enzyme was 1206 nucleotides long, and encoded a protein of 401 amino acids. Recombinant HSPH_{ZZ} was functionally overexpressed in *Escherichia coli* BL21-Codon Plus (DE3)-RIL cells and purified to homogeneity after Ni-NTA affinity chromatography. Liquid chromatography-mass spectrometry (LC-MS) analyses indicated that the enzyme could efficiently catalyze the conversion of 6-hydroxy-3-succinoylpyridine (HSP) into 2,5-dihydroxypyridine (2,5-DHP) and succinic acid in the presence of nicotinamide adenine dinucleotide (NADH) and flavin adenine dinucleotide (FAD). The kinetic constants (K_m , k_{cat} , and k_{cat}/K_m) of HSPH_{ZZ} toward HSP were 0.18 mM, 2.1 s⁻¹, and 11.7 s⁻¹ mM⁻¹, respectively. The optimum temperature, pH, and optimum concentrations of substrate and enzyme for 2,5-DHP production were 30 °C, 8.5, 1.0 mM, and 1.0 μM, respectively. Under optimum conditions, 85.3 mg/L 2,5-DHP was produced in 40 min with a conversion of 74.9%. These results demonstrated that HSPH_{ZZ} could be used for the enzymatic production of 2,5-DHP in biotechnology applications.

Keywords: HSP; 2,5-DHP; *Pseudomonas*; HSP hydroxylase; gene cloning

1. Introduction

Nicotine is the principal alkaloid in tobacco plants, and is responsible for smoking addiction and several diseases such as cancer and pulmonary disease [1–3]. The manufacturing of tobacco products and all activities involving tobacco produce large amounts of solid or liquid waste with a high nicotine content. Therefore, nicotine is the primary toxic substance in tobacco wastes [3,4]. These wastes have been designated as “toxic and hazardous wastes” under European Union Regulations [5]. Since tobacco waste is a major problem for public health and the environment, it is important to establish appropriate detoxification methods. Microbial degradation of nicotine provides a method to treat such wastes [6,7]. Several microorganisms have been found to degrade nicotine, including *Arthrobacter*, *Pseudomonas*, *Agrobacterium tumefaciens* S33, *Aspergillus oryzae*, *Sphingomonas* sp., *Acinetobacter* sp., *Shinella* sp. strain HZN7, *Rhodococcus* sp., and *Cellulomonas* sp. [3,8–14].

Recent studies have reported methods to synthesize chemicals of pharmaceutical importance from nicotine, such as (S)-macrostimine, nicotinonitrile, and fused-ring nicotine derivatives [15–18]. Dihydroxypyridines are important precursors in medicinal chemistry, and have been used to produce compounds with antitumor activity for cancer therapy, antidiabetic agents to treat

vascular disorders, and HIV protease inhibitors [19–22]. However, the lack of efficient methods to synthesize 2,5-dihydropyridine has restricted studies on its biological activity and applications [18]. The traditional chemical method to produce 2,5-dihydropyridine (2,5-DHP) is complex, creates hazardous byproducts, and has potentially undesirable side reactions and a high energy cost. Therefore, the enzymatic synthesis of 2,5-dihydropyridine represents an attractive alternative to chemical synthesis, because of its high specificity, high efficiency, and low production of pollutants.

In this study, a novel HSP (6-hydroxy-3-succinoylpyridine) hydroxylase was purified from *Pseudomonas* sp. ZZ-5 (HSPH_{ZZ}), and then its encoding gene was cloned and expressed in bacterial cells. The recombinant HSPH_{ZZ} exhibited high activity to convert HSP to 2,5-DHP. The optimum concentrations of substrate and enzyme for the formation of 2,5-DHP were determined, and the kinetic parameters and catalytic properties of the recombinant HSPH_{ZZ} were characterized.

2. Results and Discussion

2.1. Purification and Identification of HSPH_{ZZ}

The HSPH_{ZZ} with HSP hydroxylase activity was purified to homogeneity from cells of *Pseudomonas* sp. ZZ-5 using the steps shown in Table 1. The enzyme was purified 17.6-fold to give a yield of 13.4% and a specific activity of 5.1 U/mg. The molecular mass of the purified enzyme was estimated to be 45 kDa by SDS-PAGE (Figure 1), similar to that of HSP hydroxylases from *Pseudomonas putida* S16 and *Agrobacterium tumefaciens* S33 [23,24].

Table 1. Purification of a novel HSP (6-hydroxy-3-succinoylpyridine) hydroxylase from *Pseudomonas* sp. ZZ-5 (HSPH_{ZZ}).

Step	Total Protein (mg)	Total Activity (U)	Specific Activity (U/mg)	Fold	Yield (%)
Crude cell extract	672.6	195.4	0.29	1	100
(NH ₄) ₂ SO ₄ precipitation	542.3	173.5	0.31	1.1	88.8
DEAE sepharose	75.2	100.3	1.3	4.6	51.3
Phenyl sepharose	22.3	54.5	2.4	8.4	27.8
Superdex-200	5.1	26.1	5.1	17.6	13.4

Values given are the average of three replications.

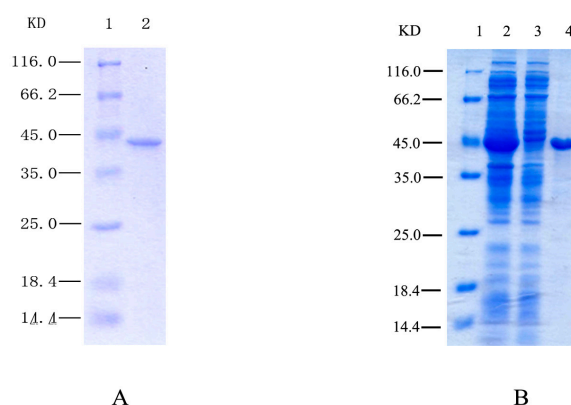


Figure 1. (A) SDS-PAGE of the purified native HSPH_{ZZ} from *Pseudomonas* sp. ZZ-5. Lane 1, molecular weight standards; Lane 2, superdex-200 gel filtration chromatography product (purified enzyme); (B) SDS-PAGE of the purified recombinant HSPH_{ZZ} from *Pseudomonas* sp. ZZ-5. Lane 1, molecular weight standards; Lane 2, crude cell extract; Lane 3, supernatant after centrifugation; Lane 4, supernatant after centrifugation; HSPH_{ZZ} after nickel affinity chromatography.

To identify the reaction catalyzed by the purified enzyme, the products of the HSPH_{ZZ} oxidation reaction were analyzed by liquid chromatography-mass spectrometry (LC-MS). The analyses of the reaction products revealed *m/z* values of 110.0, 117.1, and 194.0, which corresponded to the calculated molecular mass of 2,5-DHP (C₅H₅NO₂, 111.10), succinic acid (C₄H₆O₄, 118.09), and HSP (C₉H₉NO₄, 195.17), respectively (Supplementary Figure S1). These results demonstrated that HSPH_{ZZ} has high HSP hydroxylase activity to convert HSP to 2,5-DHP and succinic acid (Figure 2). To our knowledge, HSPH_{ZZ} is only the second example of an HSP hydroxylase from *Pseudomonas* to-date.

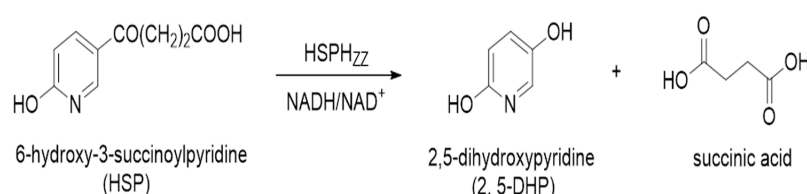


Figure 2. Enzymatic production of 2,5-dihydroxypyridine (2,5-DHP) from HSP catalyzed by the nicotine hydroxylase HSPH_{ZZ}.

2.2. Gene Cloning and Sequence Analysis of HSPH_{ZZ}

The N-terminal amino acid sequence of purified HSPH_{ZZ} was determined to be M-S-G-H-L-R-V-I-I-I-V-G-G-G-P by the automated Edman degradation technique. The DNA fragment encoding HSPH_{ZZ} was directly amplified by PCR using the genomic DNA of *Pseudomonas* sp. ZZ-5 as the template. The HSPH_{ZZ} sequence (1206 bp) was found to encode a 44.3 kDa protein composed of 401 amino acids. The amino acid sequence of HSPH_{ZZ} showed high identity with HSPHs from *P. putida* S16 (Accession No. WP_013973865.1, 86% identity), *Pseudomonas* sp. JY-Q (Accession No. WP_064613869.1, 85% identity), *Pseudomonas* sp. EGD-AK9 (Accession No. WP_031302470.1, 83% identity), and *A. tumefaciens* (Accession No. WP_031302470.1, 60% identity), respectively. Multiple sequence alignment analyses revealed that HSPH_{ZZ} contained the conserved motif Gly-Ala-Glu-Gly-Ala (amino acids 166–170), which is associated with FAD- and NAD(P)H-binding [25] (Supplementary Figure S2). At the amino acid sequence level, HSPH_{ZZ} also showed high identity to p-nitrophenol monooxygenases from *Acidovorax* sp. NO-1 (58%), *Sphingomonas melonis* TY (52%), and *Massilia putida* (43%). However, HSPH_{ZZ} did not show any detectable activity with p-nitrophenol as the substrate (data not shown).

2.3. Expression of Recombinant HSPH_{ZZ} in *Escherichia coli* BL21-Codon Plus (DE3)-RIL

The recombinant plasmid pET22b-HSPH_{ZZ} was constructed to determine the catalytic properties of recombinant HSPH_{ZZ}. The recombinant HSPH_{ZZ} was expressed in *E. coli* BL21-Codon Plus (DE3)-RIL cells and purified to homogeneity after Ni-NTA affinity and Superdex 200 gel filtration chromatography. The purified recombinant HSPH_{ZZ} with a polyhistidine (6 × His) tag at the C terminus was visible as a major band with a calculated mass of 45 kDa in SDS-PAGE analyses (Figure 1). The specific activity of the purified recombinant HSPH_{ZZ} was 31.8 U/mg—6.2-fold that of the HSPH isolated from the original strain *Pseudomonas* sp. ZZ-5 (Supplementary Table S1).

2.4. Effect of Temperature and pH on Activity of the Recombinant HSPH_{ZZ}

The effects of pH (5.5–10) and temperature (5–45 °C) on the hydroxylase activity of the recombinant HSPH_{ZZ} were determined using the standard enzyme assay. The optimum temperature and pH of HSPH_{ZZ} were determined to be 30 °C and 8.5, respectively (Figure 3). The pH optimum was higher than that of reported HSP hydroxylases from *P. putida* S16 and *A. tumefaciens* S33 (pH 8.0) [23,24]. The thermostability of HSPH_{ZZ} was evaluated at three different temperatures (30 °C, 35 °C, and 40 °C) with increasing incubation times up to 120 min. Most of the enzyme activity was maintained after incubation at 30 °C for at least 120 min, whereas incubation at 40 °C for 30 min reduced to

approximately 40% of the maximum activity. The pH stability of HSPH_{ZZ} was determined at pHs ranging from 5.5 to 10.0, and the results demonstrated that over 50% of its maximal activity was maintained from pH 7.0 to 9.0 (Supplementary Figure S3).

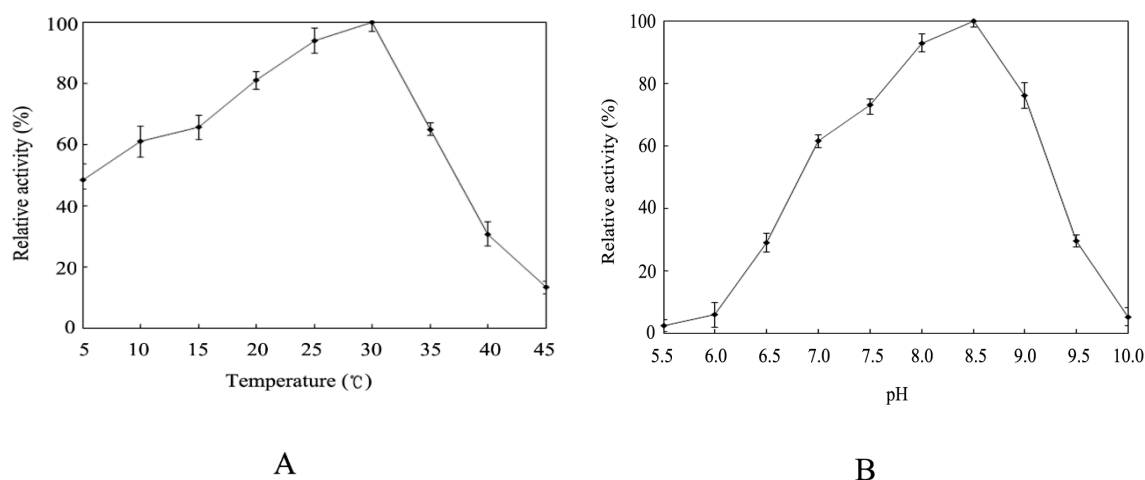


Figure 3. Temperature and pH optima of the nicotine hydroxylase HSPH_{ZZ}. (A) Temperature optimum of HSPH_{ZZ} was determined with HSP as substrates in 20 mM Tris-HCl buffer (pH 8.5) at temperatures ranging from 5 °C to 45 °C; (B) pH optimum of the enzyme at pHs ranging from 5.5 to 10 was measured for 30 min at 30 °C. The buffers used were 20 mM of sodium acetate (pH 5.5 to 6.0), sodium phosphate (pH 6.5 to 7.5), Tris-HCl (pH 8.0 to 9.0), and *N*-cyclohexyl-3-aminopropanesulfonic acid (pH 9.5 to 10.0). Relative activity was calculated by defining original activity as 100%. The values are means of three independent experiments.

2.5. Effect of Enzyme and Substrate Concentration on 2,5-DHP Production

As shown Figure 4, the effects of enzyme (0.2–2.0 μM) and substrate concentration (0.25–2.0 mM) on 2,5-DHP production were investigated. In a reaction system containing 1.0 mM HSP, the production of 2,5-DHP increased with increasing enzyme concentration from 0.2 to 1.0 μM, and then reached a plateau at about 1.0 μM. Thus, 1.0 μM was considered to be the optimum enzyme concentration for 2,5-DHP production (Figure 4). The presence of excess enzyme could result in enzyme agglomeration and diffusion problems, which could decrease the reaction efficiency [26]. The maximum production of 2,5-DHP was observed at 1 mM HSP (Figure 4). Any further increase or decrease in the HSP concentration resulted in a decrease in 2,5-DHP production. Thus, increasing the HSP concentration (from 0.25 to 1 mM) facilitated contact between the enzyme and the substrate in the reaction system [27]. The Michaelis–Menten equation was applied for catalytic kinetic analysis. The kinetic parameters of HSPH_{ZZ} for HSP were calculated under optimal conditions (at 30 °C and pH 8.5 in 20 mM Tris-HCl buffer) and a nicotinamide adenine dinucleotide (NADH) concentration of 1.0 mM. The K_m , k_{cat} , and k_{cat}/K_m of HSPH_{ZZ} for HSP were 0.18 mM, 2.1 s⁻¹, and 11.7 s⁻¹ mM⁻¹, respectively (Table 2). When the HSP concentration was 1.0 mM, the K_m , k_{cat} , and k_{cat}/K_m of HSPH_{ZZ} for NADH were 0.23 mM, 1.3 s⁻¹, and 5.7 s⁻¹ mM⁻¹, respectively (Table 2).

Table 2. Kinetic parameters of HSPH_{ZZ} for the substrate of HSP or NADH ^a.

Substrate	k_{cat} (s ⁻¹)	K_m (mM)	k_{cat}/K_m (s ⁻¹ mM ⁻¹)
HSP	2.1 ± 0.3	0.18 ± 0.04	11.7 ± 1.5
NADH	1.3 ± 0.2	0.23 ± 0.03	5.7 ± 1.1

^a The values are means of three independent experiments.

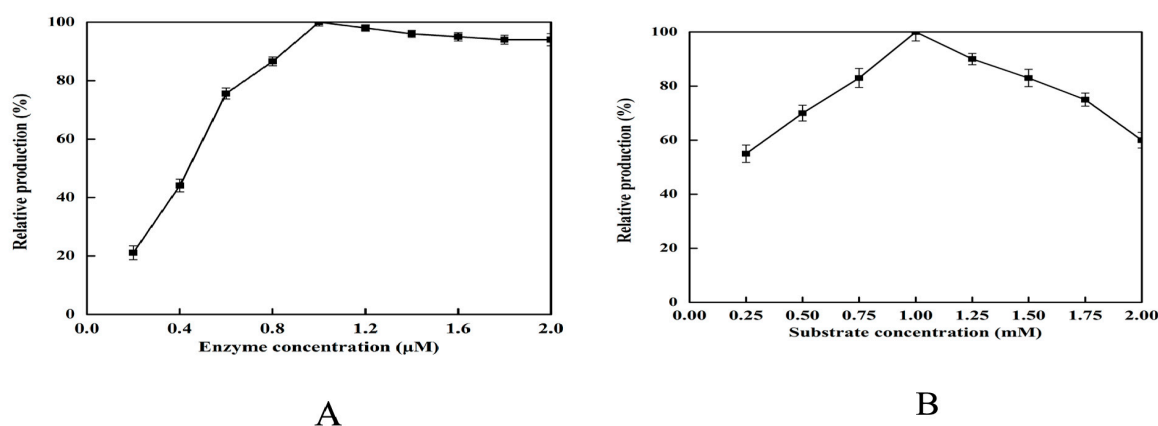


Figure 4. (A) Effect of enzyme concentration on the production of 2,5-DHP. The reactions were performed in 20 mM Tris-HCl buffer (pH 8.5) containing 10 mM FAD, 1 mM HSP, and 0.5 mM NADH at 30 °C for 30 min; (B) Effect of substrate concentration on the production of 2,5-DHP. The reactions were performed in 20 mM Tris-HCl buffer (pH 8.5) containing 10 mM FAD, 1.0 μM enzyme, and 0.5 mM NADH at 30 °C for 30 min. The values are means of three independent experiments.

2.6. Effect of Metal Ions, Organic Solvents, and Detergents on Enzymatic Activity

The effect various metal ions (Mg^{2+} , Zn^{2+} , Cu^{2+} , Ca^{2+} , Mn^{2+} , Ni^{2+} , Co^{2+} , Fe^{2+} , Na^+ , and K^+) at 5 mM on enzymatic activity was investigated by the standard enzyme assay (Table 3). The activity of HSPH_{ZZ} was not significantly affected by Mg^{2+} , Ni^{2+} , Ca^{2+} , Mn^{2+} , K^+ , Na^+ , or the chelator EDTA (0.5 mM and 5 mM), indicating that this enzyme was not a metalloprotein. However, Cu^{2+} , Co^{2+} , Zn^{2+} , and Fe^{2+} significantly inhibited enzyme activity. As shown in Table 4, the effects of methanol, acetone, formaldehyde, Dimethylformamide (DMF), chloroform, and toluene at 20% (*v/v*) also markedly inhibited enzyme activity, while more than 90% of HSPH_{ZZ} activity was retained after incubation with DMSO. Incubation with Triton X-100, Span 20, and Span 40 at 1% (*w/v*) reduced the hydroxylase activity by less than 50% (Table 4). The enzyme activity was not reduced by adding Tween 20, Tween 40, or Tween 80 at 1% (*w/v*).

Table 3. Effect of various metals on the enzymatic activity of HSPH_{ZZ}^a.

Metals or Inhibitors	Concentration	Relative Activity (%)
None	-	100
Mg^{2+}	5 mM	86 ± 3
Zn^{2+}	5 mM	27 ± 2
Cu^{2+}	5 mM	23 ± 1
Ca^{2+}	5 mM	92 ± 2
Mn^{2+}	5 mM	87 ± 4
Fe^{2+}	5 mM	13 ± 2
Ni^{2+}	5 mM	81 ± 3
Co^{2+}	5 mM	31 ± 3
K^+	5 mM	101 ± 5
Na^+	5 mM	98 ± 2
EDTA	0.5 mM	79 ± 2
	5 mM	85 ± 2

^a The values are means of three independent experiments.

Table 4. Effect of various organic solvent and detergents on the activity of HSPH_{ZZ} ^a.

Metals or Inhibitors	Concentration (%)	Relative Activity (%)
None	—	100
Methanol	20 (v/v)	61 ± 2
Acetone	20 (v/v)	59 ± 4
Chloroform	20 (v/v)	33 ± 2
Formaldehyde	20 (v/v)	23 ± 3
Toluene	20 (v/v)	28 ± 5
DMF	20 (v/v)	65 ± 2
DMSO	20 (v/v)	93 ± 5
Tween 20	1 (w/v)	86 ± 5
Tween 40	1 (w/v)	110 ± 4
Tween 80	1 (w/v)	91 ± 1
Triton X-100	1 (w/v)	48 ± 3
Span 20	1 (w/v)	12 ± 4
Span 40	1 (w/v)	17 ± 5

^a The values are means of three independent experiments.

2.7. 2,5-DHP Production from HSP by HSPH_{ZZ} under Optimum Conditions

The production of 2,5-DHP from HSP by HSPH_{ZZ} was investigated under optimum conditions (at 30 °C and pH 8.5 in 20 mM Tris-HCl buffer), with HSPH_{ZZ} at a concentration of 1 µM in the standard enzyme assay. The enzyme produced 2,5-DHP (85.3 mg/L) in 40 min with a conversion of 74.9% (w/w) (Figure 5). The 2,5-DHP decomposed over time in the reaction solution, indicating that it was unstable and probably sensitive to oxidation. The amount of HSP consumed in the enzyme reaction in 40 min was 161 mg/L (0.83 mM) out of the initial 200 mg/L. Based on the conversion stoichiometry, the estimated amount of 2,5-DHP produced was 92.1 mg/L, corresponding to a conversion yield of 80.9%. Thus, the amount of 2,5-DHP lost during the reaction was 6.8 mg/L (amount produced minus amount detected). The rate of HSP catalysis by HSPH_{ZZ} was higher than that of the HSP hydroxylase from *A. tumefaciens* S33 (69.7% at 35 °C and pH 8.0 in 50 min) [28]. These results demonstrated that HSPH_{ZZ} has strong activity to produce 2,5-DHP HSP, making it a potential candidate for enzymatic transformation of HSP into 2,5-DHP in commercial applications.

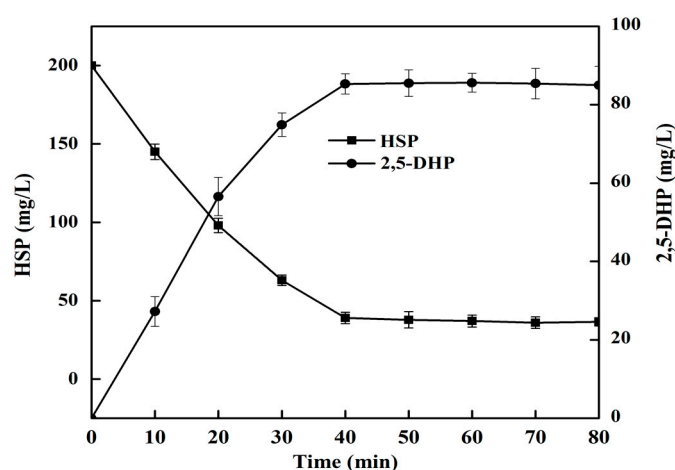


Figure 5. Time course of 2,5-DHP (circles) production from HSP (boxes) under the optimum condition. The reactions were performed in 20 mM Tris-HCl buffer (pH 8.5) containing 10 mM FAD, 1.0 µM enzyme, 200 mg/L HSP, and 0.5 mM NADH at 30 °C for 80 min. The values are means of three independent experiments.

3. Experimental Section

3.1. Chemicals, Strains, and Plasmids

Using nicotine as the sole source of carbon and nitrogen, *Pseudomonas* sp. ZZ-5 was isolated from soil samples obtained from a field under continuous tobacco cropping in Henan, P.R. China. The strain was cultured in nicotine medium containing (per liter) 22.8 g $K_2HPO_4 \cdot 3H_2O$, 6.8 g KH_2PO_4 , 0.5 g $MgSO_4 \cdot 7H_2O$, and 1 mL trace elements solution. The trace elements solution contained 0.05 g $CaCl_2 \cdot 2H_2O$, 0.05 g $CuCl_2 \cdot 2H_2O$, 0.008 g $MnSO_4 \cdot H_2O$, 0.004 g $FeSO_4 \cdot 7H_2O$, 0.1 g $ZnSO_4$, 0.1 g $Na_2MoO_4 \cdot 2H_2O$, and 0.05 g $Na_2WO_4 \cdot 2H_2O$ [9,29]. The plasmid pET22b and *E. coli* strain BL21-CodonPlus (DE3)-RIL were respectively bought from Novagen (Madison, WI, USA) and Stratagene (La Jolla, CA, USA). Pyrobest DNA polymerase, restriction enzymes, and the DNA ligation kit were purchased from Takara Biotechnology (Dalian, China). The DEAE-anion exchange column, phenyl-sepharose column, nickel columns, and Superdex 200 gel filtration columns were from GE Healthcare (Buckinghamshire, UK), and 2,5-DHP was purchased from SynChem OHG (Altenburg, Germany). Chromatographic-grade succinic acid was purchased from J&K Scientific Ltd. (Beijing, China). We obtained HSP from Professor Hongzhi Tang at Shanghai Jiao Tong University. All other chemicals were of analytical grade and were obtained from Sangon (Shanghai, China).

3.2. Purification of HSP_{HZZ}

Cells of *Pseudomonas* sp. ZZ-5 (approx. 15 g) were suspended in 50 mM Tris-HCl buffer (pH 8.0) and disrupted by sonication (40 kHz, 80–100 W). The supernatant was subjected to ammonium sulfate fractionation and yielded a precipitate at 50–70% saturation with $(NH_4)_2SO_4$. The mixture was allowed to stand overnight, and then the precipitate was collected by centrifugation at $20,000 \times g$ for 20 min. The precipitate was loaded onto a DEAE-anion exchange column ($1 \times 20 \text{ cm}^2$, GE Healthcare) equilibrated with 50 mM Tris-HCl buffer (pH 8.0). The column was washed with a linear salt gradient from 50 mM to 1 M NaCl. The fractions containing the target protein were collected at 300–400 mM and concentrated using a membrane with a 30-kDa MW cut off. The sample was applied to a phenyl-sepharose column ($1 \times 20 \text{ cm}^2$, GE Healthcare, Buckinghamshire, UK) equilibrated with 50 mM Tris-HCl buffer containing 1.0 M $(NH_4)_2SO_4$. The target protein was eluted at an $(NH_4)_2SO_4$ concentration of 0.8 M, desalted, and then enriched. Finally, the protein mixture was loaded onto a Superdex 200 gel filtration column (GE Healthcare, Buckinghamshire, UK), which was pre-equilibrated with 50 mM Tris-HCl (pH 8.0) containing 200 mM NaCl. The fraction size was 1 mL (flow rate, 1 mL/min). The peak fractions were determined by assaying enzymatic activity under standard conditions. The fractions with HSP hydroxylase activity were collected and analyzed by SDS-PAGE. The protein concentration was determined using the Bradford method.

3.3. Enzymatic Activity Assay

The activity of HSP hydroxylase was determined using the method of Tang et al. [23,30]. The standard reaction mixture, containing 10 mM FAD, 1 mM HSP, 0.5 mM NADH, and 20 mM Tris-HCl buffer (pH 8.5), was preincubated for 2 min and then the reaction was started by adding the purified enzyme. The enzymatic activity was measured at 30 °C for 30 min and the production of 2,5-DHP was monitored by liquid chromatography-mass spectrometry (LC-MS) analysis. The reaction products were characterized by an electron spray ionization (ESI) source on an AB Sciex Triple Quad 5500 mass spectrometer with an Agilent 1290 infinity LC system for UHPLC. The UHPLC analyses were performed with a ZORBAX Eclipse Plus-C18 column (column size, $150 \times 4.6 \text{ mm}$; particle size, 5 μm ; Agilent, Palo Alto, CA, USA) and a mobile phase of methanol:1 mM acetic acid (25:75, v/v; flow rate, 0.5 mL/min).

One unit of hydroxylase activity was defined as the amount of enzyme releasing 1 mol 2,5-DHP per min under standard conditions. Measurements were corrected for background hydrolysis in the absence of enzyme.

3.4. N-Terminal Amino Acid Sequence of HSPH_{ZZ}

After analysis by SDS-PAGE, the target protein was transferred onto a polyvinylidene difluoride membrane Hybond-P (Amersham Pharmacia Biotech, Orsay, France) and visualized with Coomassie brilliant blue staining. Then, the corresponding bands were excised, and the N-terminal and internal partial amino acid sequences of the protein were determined by the Sangon.

3.5. Gene Cloning and Construction of Expression Plasmid

The N-terminal amino acid sequence of HSPH_{ZZ} was used to search the GenBank database, and the sequences retrieved were used to design primers to amplify HSPH_{ZZ}. The gene encoding HSPH_{ZZ} was amplified using PCR with the following primers: forward, 5'-GCACATATGAGCGG ACATCAGGATGTCATC-3', and reverse, 5'-GCGGTCGACCAACTATGTCTGCATTAATTGCGG-3' (NdeI and SalI sites underlined, respectively). Genomic DNA was extracted from *Pseudomonas* sp. ZZ-5 using a Gentra Puregene Yeast/bact. Kit B following the manufacturer's instructions (Qiagen, Valencia, CA, USA) and used as the template for PCR amplification. The PCR conditions were as follows: 94 °C for 1 min, 60 °C for 1 min, 72 °C for 2 min, and a final extension at 72 °C for 10 min. The PCR product was subsequently purified, digested with NdeI and SalI, and then cloned into pET22b to generate pET15b-HSPH_{ZZ}. The DNA insert was sequenced to confirm that no unintended mutation had occurred.

3.6. Expression and Purification of Recombinant HSPH_{ZZ}

The plasmid pET15b-HSPH_{ZZ} was transformed into *E. coli* BL21-Codon Plus (DE3)-RIL cells for gene expression. The transformed cells were grown in LB broth containing 100 mg/L ampicillin and 34 mg/L chloramphenicol at 37 °C and with shaking at 150 rpm. When the OD₆₀₀ value of the cultures reached 0.4–0.6, isopropyl-β-D-thiogalactopyranoside (IPTG) was added to a final concentration of 0.2 mM to induce gene expression. After further culture for 6 h at 30 °C, the cells were harvested by centrifugation, resuspended in buffer A (50 mM Tris-HCl, pH 7.8, 200 mM NaCl) and disrupted by sonication. Cell debris was removed by centrifugation at 20,000× g at 4 °C for 20 min. The soluble fraction was loaded onto a Ni²⁺-NTA agarose column (GE Healthcare, Buckinghamshire, UK) pre-equilibrated with buffer A. After washing with buffer containing 60 mM imidazole, the enzymes were eluted with buffer B (20 mM Tris-HCl, pH 7.8, 500 mM NaCl, 300 mM imidazole). The purified protein was analyzed by SDS-PAGE (12% polyacrylamide) and the protein concentration was determined using the Bradford method.

3.7. Catalytic Properties of Recombinant HSPH_{ZZ}

The optimum pH and temperature for recombinant HSPH_{ZZ} activity were determined using the standard enzymatic assay and LC-MS (AB Sciex, Framingham, MA, USA). The effect of pH on hydroxylase activity was examined at 30 °C within the pH range of 5.5 to 10.0. The effect of temperature (from 5 °C to 45 °C) on enzymatic activity was investigated at pH 8.5. The effects of several different metal ions, organic solvents, and detergents on the activity of HSPH_{ZZ} were determined by adding each metal salt (5 mM), organic solvent (20%, v/v), and detergent (1%, v/v) to the standard assay solution.

4. Conclusions

We have cloned a novel HSP hydroxylase from *Pseudomonas* sp. ZZ-5 (HSPH_{ZZ}), and expressed it in a bacterial cell system. The recombinant HSPH_{ZZ} showed strong enzymatic activity to convert HSP to 2,5-DHP in the presence of NADH and FAD. The effects of temperature, pH, and concentrations of substrate and enzyme for 2,5-DHP production were optimized. Under optimum conditions, HSPH_{ZZ} produced 85.3 mg/L 2,5-DHP from 200 mg/L of HSP in 40 min with a conversion rate of 74.9%. These results demonstrate that HSPH_{ZZ} could be a potential candidate for the enzymatic synthesis of 2,5-DHP in pharmaceutical applications.

Supplementary Materials: The following are available online at www.mdpi.com/2073-4344/7/9/257/s1, Figure S1: LC-MS profiles of the reaction catalyzed by HSPH_{ZZ}. Mass spectra of products succinic acid (m/z 117.15) (a), 2,5-DHP (m/z 110.18) (b) and substrate HSP (m/z 194.04) (c), respectively. Negatively charged ions were detected; Figure S2: Multiple sequence alignment for HSPH_{ZZ} and its homologs. An alignment was carried out using Clustal W program with manual adjusting. The conserved GADGA motif is in shallow. Abbreviation: HSPH_{ZZ} from *Pseudomonas* sp. ZZ-5; WP_013973865.1 from *Pseudomonas putida* S16; WP_031302470.1 from *Pseudomonas* sp. EGD-AK9; WP_064613869.1 from *Pseudomonas* sp. JY-Q; WP_035209888.1 from *Agrobacterium tumefaciens* S33; Figure S3: Thermal stability (A) and pH stability (B) of HSPH_{ZZ}. A. Thermal stability of HSPH_{ZZ}. The residual enzyme activity was measured after incubation of the purified enzyme at 30 °C (triangles), 35 °C (boxes), and 40 °C (diamonds), respectively. B. pH stability of the enzyme at pHs ranging from 5.5 to 10 was measured for 30 min at 30 °C. The values are means of three independent experiments. Table S1: Purification of the recombinant HSPH_{ZZ} from *Pseudomonas* sp. ZZ-5.

Acknowledgments: This work was supported by grants from the Henan Province Foreign Cooperation Projects (152106000058), key scientific and technological project of Henan Province (162102210061) and the National Natural Science Foundation of China (21406210).

Author Contributions: T.W. designed and performed the experiments, analyzed the data and prepared the manuscript. J.Z., Y.Z., H.T. and S.H. assisted in data analysis. D.M. performed experiments, analyzed the data and assisted in manuscript preparation. All authors read and approved the final manuscript.

Conflicts of Interest: The authors declare no conflict of interest.

References

- Benowitz, N.L. Nicotine addiction. *N. Engl. J. Med.* **2010**, *362*, 2295–2303. [[CrossRef](#)] [[PubMed](#)]
- Hecht, S.S. Tobacco smoke carcinogens and lung cancer. *J. Natl. Cancer Inst.* **1999**, *91*, 1194–1210. [[CrossRef](#)] [[PubMed](#)]
- Civilini, M.; Domenis, C.; Sebastianutto, N.; de Bertoldi, M. Nicotine decontamination of tobacco agro-industrial waste and its degradation by micro-organisms. *Waste Manag. Res.* **1997**, *15*, 349–358. [[CrossRef](#)]
- Novotny, T.E.; Zhao, F. Consumption and production waste: Another externality of tobacco use. *Tob. Control* **1999**, *8*, 75–80. [[CrossRef](#)] [[PubMed](#)]
- Seckar, J.A.; Stavanja, M.S.; Harp, P.R.; Yi, Y.; Garner, C.D.; Doi, J. Environmental fate and effects of nicotine released during cigarette production. *Environ. Toxicol. Chem.* **2008**, *27*, 1505–1514. [[CrossRef](#)] [[PubMed](#)]
- Wang, J.H.; He, H.Z.; Wang, M.Z.; Wang, S.; Zhang, J.; Wei, W.; Xu, H.X.; Lu, Z.M.; Shen, D.S. Bioaugmentation of activated sludge with *Acinetobacter* sp. TW enhances nicotine degradation in a synthetic tobacco wastewater treatment system. *Bioresour. Technol.* **2013**, *142*, 445–453. [[CrossRef](#)] [[PubMed](#)]
- Zhong, W.; Zhu, C.; Shu, M.; Sun, K.; Zhao, L.; Wang, C.; Ye, Z.; Chen, J. Degradation of nicotine in tobacco waste extract by newly isolated *Pseudomonas* sp. ZUTSKD. *Bioresour. Technol.* **2010**, *101*, 6935–6941. [[CrossRef](#)] [[PubMed](#)]
- Ruan, A.D.; Min, H.; Zhu, W. Studies on biodegradation of nicotine by *Arthrobacter* sp. strain HF-2. *J. Environ. Sci. Health B* **2006**, *41*, 1159–1170. [[CrossRef](#)] [[PubMed](#)]
- Wang, S.N.; Xu, P.; Tang, H.Z.; Meng, J.; Liu, X.L.; Huang, J.; Chen, H.; Du, Y.; Blankespoor, H.D. Biodegradation and detoxification of nicotine in tobacco solid waste by a *Pseudomonas* sp. *Biotechnol. Lett.* **2004**, *26*, 1493–1496. [[CrossRef](#)] [[PubMed](#)]
- Wang, M.Z.; Yang, G.Q.; Min, H.; Lv, Z.M. A novel nicotine catabolic plasmid pMH1 in *Pseudomonas* sp. strain HF-1. *Can. J. Microbiol.* **2009**, *55*, 228–233. [[CrossRef](#)] [[PubMed](#)]
- Qiu, J.G.; Ma, Y.; Wen, Y.Z.; Chen, L.S.; Wu, L.F.; Liu, W.P. Functional identification of two novel genes from *Pseudomonas* sp. strain HZN6 involved in the catabolism of nicotine. *Appl. Environ. Microbiol.* **2012**, *78*, 2154–2160. [[CrossRef](#)] [[PubMed](#)]
- Meng, X.J.; Lu, L.L.; Gu, G.F.; Xiao, M. A novel pathway for nicotine degradation by *Aspergillus oryzae* 112822 isolated from tobacco leaves. *Res. Microbiol.* **2010**, *161*, 626–633. [[CrossRef](#)] [[PubMed](#)]
- Qiu, J.G.; Li, N.; Lu, Z.M.; Yang, Y.J.; Ma, Y.; Niu, L.L.; He, J.; Liu, W.P. Conversion of nornicotine to 6-hydroxy-nornicotine and 6-hydroxy-myosmine by *Shinella* sp. strain HZN7. *Appl. Microbiol. Biotechnol.* **2016**, *100*, 10019–10029. [[CrossRef](#)] [[PubMed](#)]
- Wang, M.Z.; Yang, G.Q.; Wang, X.; Yao, Y.L.; Min, H.; Lu, Z.M. Nicotine degradation by two novel bacterial isolates of *Acinetobacter* sp. TW and *Sphingomonas* sp. TY and their responses in the presence of neonicotinoid insecticides. *World J. Microbiol. Biotechnol.* **2011**, *27*, 1633–1640. [[CrossRef](#)]

15. Enamorado, M.F.; Ondachi, P.W.; Comins, D.L. A five-step synthesis of (*S*)-macrostomine from (*S*)-nicotine. *Org. Lett.* **2010**, *12*, 4513–4515. [[CrossRef](#)] [[PubMed](#)]
16. Ondachi, P.W.; Comins, D.L. Synthesis of fused-ring nicotine derivatives from (*S*)-nicotine. *J. Org. Chem.* **2010**, *75*, 1706–1716. [[CrossRef](#)] [[PubMed](#)]
17. Kagarlitskii, A.D.; Iskakova, M.K.; Turmukhambetov, A.Z. Catalytic conversion of nicotine into nicotinonitrile—a pharmaceutical intermediate product. *Pharm. Chem. J.* **2002**, *36*, 26–27. [[CrossRef](#)]
18. Fananas, F.J.; Arto, T.; Mendoza, A.; Rodriguez, F. Synthesis of 2,5-dihydropyridine derivatives by gold-catalyzed reactions of β -ketoesters and propargylamines. *Org. Lett.* **2011**, *13*, 4184–4187. [[CrossRef](#)] [[PubMed](#)]
19. Abbas, H.A.S.; El Sayed, W.A.; Fathy, N.M. Synthesis and antitumor activity of new dihydropyridine thioglycosides and their corresponding dehydrogenated forms. *Eur. J. Med. Chem.* **2010**, *45*, 973–982. [[CrossRef](#)] [[PubMed](#)]
20. Briede, J.; Stivrina, M.; Vigante, B.; Stoldere, D.; Duburs, G. Acute effect of antidiabetic 1,4-dihydropyridine compound cerebrocrast on cardiac function and glucose metabolism in the isolated, perfused normal rat heart. *Cell Biochem. Chem. Funct.* **2008**, *26*, 238–245. [[CrossRef](#)] [[PubMed](#)]
21. Kappe, C.O. Biologically active dihydropyrimidones of the Biginelli-type—A literature survey. *Eur. J. Med. Chem.* **2000**, *35*, 1043–1052. [[CrossRef](#)]
22. Hilgeroth, A. Dimeric 4-aryl-1,4-dihydropyridines: Development of a third class of nonpeptidic HIV-1 protease inhibitors. *Mini-Rev. Med. Chem.* **2002**, *2*, 235–245. [[CrossRef](#)] [[PubMed](#)]
23. Tang, H.Z.; Yao, Y.X.; Zhang, D.K.; Meng, X.Z.; Wang, L.J.; Yu, H.; Ma, L.Y.; Xu, P. A novel NADH-dependent and FAD-containing hydroxylase is crucial for nicotine degradation by *Pseudomonas putida*. *J. Biol. Chem.* **2011**, *286*, 39179–39187. [[CrossRef](#)] [[PubMed](#)]
24. Wang, S.; Huang, H.; Xie, K.; Xu, P. Identification of nicotine biotransformation intermediates by *Agrobacterium tumefaciens* strain S33 suggests a novel nicotine degradation pathway. *Appl. Microbiol. Biotechnol.* **2012**, *95*, 1567–1578. [[CrossRef](#)] [[PubMed](#)]
25. Eppink, M.H.; Schreuder, H.A.; Van Berkel, W.J. Identification of a novel conserved sequence motif in flavoprotein hydroxylases with a putative dual function in FAD/NAD(P)H binding. *Protein Sci.* **1997**, *6*, 2454–2458. [[CrossRef](#)] [[PubMed](#)]
26. Li, H.L.; Xie, K.B.; Huang, H.Y.; Wang, S.N. 6-Hydroxy-3-Succinoylpyridine hydroxylase catalyzes a central step of nicotine degradation in *Agrobacterium tumefaciens* S33. *PLoS ONE* **2014**, *9*, e103324. [[CrossRef](#)] [[PubMed](#)]
27. Wei, T.; Huang, S.; Zang, J.; Jia, C.X.; Mao, D.B. Cloning, expression and characterization of a novel fructosyltransferase from *Aspergillus oryzae* ZZ-01 for the synthesis of sucrose 6-acetate. *Catalysts* **2016**, *6*, 67. [[CrossRef](#)]
28. Yang, Z.; Pan, W.B. Ionic liquids: Green solvents for nonaqueous biocatalysis. *Enzym. Microb. Technol.* **2005**, *37*, 19–28. [[CrossRef](#)]
29. Wang, S.N.; Liu, Z.; Tang, H.Z.; Meng, J.; Xu, P. Characterization of environmentally friendly nicotine degradation by *Pseudomonas putida* biotype A strain S16. *Microbiology* **2007**, *153*, 1556–1565. [[CrossRef](#)] [[PubMed](#)]
30. Yu, H.; Hausinger, R.P.; Tang, H.Z.; Xu, P. Mechanism of the 6-Hydroxy-3-succinoyl-pyridine 3-monooxygenase flavoprotein from *Pseudomonas putida* S16. *J. Biol. Chem.* **2014**, *289*, 29158–29170. [[CrossRef](#)] [[PubMed](#)]

